

Hf isotope ratio analysis using multi-collector inductively coupled plasma mass spectrometry: an evaluation of isobaric interference corrections

Nan-Chin Chu,^{*a} Rex N. Taylor,^a Valérie Chavagnac,^a Robert W. Nesbitt,^a Rose M. Boella,^a J. Andrew Milton,^a Christopher R. German,^a Germain Bayon^b and Kevin Burton^b

^aSouthampton Oceanography Centre, Southampton SO14 3ZH, UK.

E-mail: nxc@soc.soton.ac.uk; Fax: 44-23-80596554; Tel: 44-23-80596563

^bDepartment of Earth Sciences, The Open University, Walton Hall, Milton Keynes, MK7 6AA, UK

www.rsc.org/jaas

Received 10th July 2002, Accepted 6th November 2002

First published as an Advance Article on the web 18th November 2002

From measurements of Hf–Yb mixtures, we have found that the correction of isobaric interferences involving accepted Yb isotope ratios and reasonable estimates of mass bias result in a significantly under-corrected ^{176}Hf , which is proportional to the amount of Yb added. This can be explained by (1) a significant difference in the instrumental mass bias between Hf and Yb, and (2) that the accepted values for isotopic ratios within the Yb and/or Hf systems are incorrect. We have evaluated these possibilities by measuring mixed solutions of Yb and Hf on two MC-ICP-MS instruments and undertaking a series of REE fractionation experiments using a thermal ionisation mass spectrometer (TIMS). Our results indicate that the presently accepted abundances of the Yb isotopes are not appropriate. We present new values for Yb isotopic abundances based on the TIMS and MC-ICP-MS results. Using the newly defined Yb values, we demonstrate that Yb and Hf have similar levels of mass bias in plasma ionisation instruments, and that Hf isotope ratios can be used to correct Yb mass bias before subsequent correction of isobaric interference. A laser ablation comparison of Yb and Hf indicates that similar relationships exist, and can be applied to micro-analytical techniques where chemical separation is not possible.

Introduction

Hafnium isotope studies have increased in number since the advent of plasma source mass spectrometry, which, unlike traditional thermal ionisation mass spectrometry (TIMS), overcomes the difficulties of elements with high first ionisation potential. Most analytical protocols and correction procedures for MC-ICP-MS are directly transferred from TIMS. However, as the mass bias of a multi-collector ICP-MS is about 10 times that of a TIMS, it has been suggested¹ that the mass bias behaviour should be better characterised, especially where isobaric interferences need to be corrected. This is particularly true where hafnium purification is not possible prior to sample introduction to MC-ICP-MS. For example, the laser ablation of solid samples frequently involves coincident ionisation of the REE. Yb thus introduced results in isobaric ^{176}Yb interference on the radiogenic ^{176}Hf , which is the isotope of interest in the hafnium system. As such, the correction of isobaric interferences needs to be rigorously constrained to achieve a satisfactory accuracy of Hf isotope ratios.

It has been suggested that the extent of mass bias in plasma source instruments varies with mass in a coherent fashion.^{2,3} Therefore, it should be plausible to use the mass bias determined for isotopes of one element to correct externally the isotopic mass bias of an element with similar mass (e.g., Tl–Pb² and Zn–Cu³). It is also recognised that even neighbouring elements are not biased to exactly the same extent but that the relative mass bias remains constant over one measurement session.^{3,4} To achieve high precision and better accuracy these authors have applied a modified correction based on the correlation between the mass bias of element pairs. For isotopic systems with well-determined and invariant isotope pairs, the

magnitude of mass bias during a run can be assessed (e.g., $^{146}\text{Nd}/^{144}\text{Nd}$ and $^{179}\text{Hf}/^{177}\text{Hf}$) and the calculated instrumental bias applied to radiogenic isotopes of interest and to relevant isobaric interferences.^{5,6} If differences exist between the level of ionisation of element pairs in a plasma, as proposed by Maréchal *et al.* (1999) and White *et al.* (2000), better constraints on inter-element mass bias are needed to correct isobaric interferences, especially where interfering element/object element ratios are high.

^{176}Yb is a major isobaric interference that has to be corrected by monitoring another Yb isotope, e.g. ^{171}Yb or ^{173}Yb , during a Hf measurement. Some previous laser ablation studies^{7,8} have argued that the accepted isotopic abundances of Yb^{9,10} do not result in a consistently corrected $^{176}\text{Hf}/^{177}\text{Hf}$ ratio. Such studies have modified the values by empirically deriving a correction by generating a suitable Yb isotope ratio, which results in a consistent $^{176}\text{Hf}/^{177}\text{Hf}$. This method is limited by the assumption that the Yb mass bias is consistent between the empirically derived solution and the sample measurements. In reality, the degree of bias is likely to vary with the nature of the sample matrix and through time.

In this study, we have evaluated the possible pitfalls in Hf isotope measurements on different instruments in order to achieve accurate results even with high levels of interference.

Experimental

Chemistry separation

The Hf separation method used at the Southampton Oceanography Centre (SOC) and The Open University is derived from two previously published methods.^{11,12} Its purpose is to

separate Hf rapidly and efficiently from isobaric and non-isobaric interfering elements, *e.g.* Yb and Ti. Two columns are employed for this separation scheme, anion exchange resin AG1-X8 (Bio-Rad) and EICHRON[®] Ln-resin (Table 1).

Ti in the analyte suppresses the ionisation of Hf, and thus Ti needs to be removed from the sample such that the Ti concentration is less than 1 µg g⁻¹ in the measurement solution.¹³ The use of hydrogen peroxide, which raises the oxidation state of Ti and forms the yellow-tinted peroxytitanyl compound Ti(O-O)²⁺, results in a satisfactory separation of Hf and Ti. 1% of H₂O₂ is added to the HCl in the second column eluate (Table 1). The collected fraction from the second column is converted to a 2% HNO₃ matrix for analysis. The recovery of this chemical separation is generally about 90%.

Instrumentation and measurement systematics

Two different types of MC-ICP-MS have been used to measure Hf isotopes in this study: an IsoProbe (Micromass Ltd., UK) at Southampton Oceanography Centre and a Nu Plasma (Nu Instruments, Wrexham, UK) at The Open University. Details

of these two instruments have been described elsewhere.^{14,15} All standards and samples were prepared with 2% HNO₃ and introduced *via* two types of desolvating nebulizers, the MCN 6000 and the Aridus (both from CETAC, Omaha, NB, USA) for the IsoProbe and the Nu Plasma, respectively. The normal operating conditions of the two instruments are summarised in Table 2.

Hf isotopes on the IsoProbe and Nu Plasma are measured statically in the Faraday collector arrays shown in Table 3. Various collector configurations were examined with the JMC 475 Hf standard on the IsoProbe; the results were indistinguishable within the error of the measurements (Table 4). This suggests that there are negligible differences between the collector efficiencies of each Faraday collector and justifies the use of static analysis. In both instruments, collectors were set to measure both ¹⁷¹Yb and ¹⁷³Yb to calculate the ¹⁷⁶Yb interference on ¹⁷⁶Hf and to determine the mass bias of Yb isotopes (detailed below). On the IsoProbe, the collector positions were checked before each analytical session using a mixed solution of Hf, Lu and Yb (Hf at ~12 ng ml⁻¹, Lu at ~1 ng ml⁻¹ and Yb at ~0.1 ng ml⁻¹). On the Nu Plasma, the

Table 1 Hf ion-exchange column specification and elution profile (after refs. 6 and 12)

Resin type	Column dimension	Eluent	Elements
Bio-Rad AG1-X8 (200–400 mesh)	4 cm height 0.8 cm ø	Sample in 2 ml 4 M HF Elute 8 ml 4 M HF Collect 8 ml 6 M HCl: 1 M HF	Bulk Matrix Ti, Zr, Hf ± HREE
Eichrom Ln (100–150 µm)	8.3 cm height 0.4 cm ø	Sample in 100 µl 2.2 M HCl : 1% H ₂ O ₂ Elute 200 µl 2.2 M HCl : 1% H ₂ O ₂ Elute 3.7 ml 2.2 M HCl : 1% H ₂ O ₂ Elute 12 ml 6 M HCl Collect 6 ml 1 M HF	Ti, Zr, Hf Ti Ti HREE Hf and Zr

Table 2 Operating conditions of the Micromass IsoProbe and Nu Plasma for Hf measurement

	IsoProbe	Nu Plasma
Argon gas flow rates		
Cool gas	14.0 l min ⁻¹	13.0 l min ⁻¹
Auxiliary gas	1.0 l min ⁻¹	1.0 l min ⁻¹
Nebuliser gas	1.05 l min ⁻¹	0.1 min ⁻¹
Collision gas flow rate (Ar)	1.2 ml min ⁻¹	N/A
Nebuliser type	Cetac MCN 6000	Cetac Aridus
Spray chamber temperature	75 °C	70 °C
Desolvator temperature	160 °C	160 °C
N ₂ gas flow	0.10 l min ⁻¹	0.07–0.11 l min ⁻¹
Sweep gas flow (Ar)	2.25–2.60 l min ⁻¹	3.00–3.75 l min ⁻¹
Solution uptake rate	60 µl min ⁻¹	50 µl min ⁻¹
Forward (rf) power	1350 W	1300 W
Interface cones	Nickel	Nickel
Analyser vacuum	3 × 10 ⁻⁸ Pa	5 × 10 ⁻⁹ Pa
Acceleration voltage	5.5 kV	4.0 kV
Ion lens setting (IsoProbe)/ Focusing Optics (Nu)	Optimised for maximum intensity with extract (Ex) focusing at 35%	Optimised for maximum intensity
Detector used	9 Faraday collectors	10 Faraday collectors
Typical Hf sensitivity	300 V ppm ⁻¹	130 V ppm ⁻¹
Sampling time	4 blocks of 25 ratios (~12 min)	4 blocks of 25 ratios (~10 min)
Typical Hf introduced (ng)/analysis	28 ng	30 ng

Table 3 Faraday collector array scheme of the IsoProbe and Nu Plasma, typical baseline signals and elemental abundances

IsoProbe	Faraday collector	L3	L2	Axial	H1	H2	H3	H4	H5	H6	F2	F1
Nu Plasma	Faraday collector	F10	F9	N/A	F8	F7	F6	F5	F4	F3		
	<i>m/z</i> measure	171	173	174	175	176	177	178	179	180	181	183
	Abundance ^a	Yb 14.28%	Lu 16.13%	Hf 31.83%	Ta 97.41%	W 2.59%						
				0.16%		5.26%	18.60%	27.28%	13.62%	35.08%	99.98%	14.31%
										0.01%		

^aTUPAC Commission on Atomic Weights and Isotopic Abundances report in 'Isotopic Compositions of the Elements 1997', *Pure Appl. Chem.*, 1998, **70**(1), 217.

Table 4 Various static mode collector configurations and corresponding JMC475 ratio measurements

IsoProbe										
Faraday	L3	L2	Axial	H1	H2	H3	H4	H5	H6	$^{176}\text{Hf}/^{177}\text{Hf} \pm 2 \text{ sd}$ (no. of analyses)
	171	173	175	176	177	178	179	180	181	0.282162 ± 24 (55)
m/z measure	171	173	174	175	176	177	178	179	180	0.282168 ± 33 (21)
		171	173	174	175	176	177	178	179	0.282165 ± 5 (4)

zoom lens system was set at the values determined to accommodate the dispersion of the Hf isotopes amongst the fixed collectors. The beam intensities of both instruments were then optimised by adjusting the torch position, gas flows, ion focusing and magnet field settings. The overall input/output efficiency, *i.e.*, the final ion current measured relative to the amount of Hf introduced, was 0.5% for the IsoProbe and 0.2% for the Nu Plasma.

The collector baselines were measured on-peak on the IsoProbe using the same 2% HNO_3 used for the sample matrix. These baselines were then subtracted from the appropriate peaks of subsequent standard or sample measurements. On the Nu Plasma, the baseline was measured at half masses and corrected on-line during each measurement. For both instruments, the sample analysis baselines were remeasured after cleaning the sample introduction system with 10% HNO_3 , 1% HF, MQ (high purity deionised water) and isopropyl alcohol (IPA) for 15 min, followed by 5 min of equilibration in 2% HNO_3 . Following the cleaning procedure no differences were detected between the on-peak 2% HNO_3 baselines and the instrument baselines.

Laser ablation analyses on the IsoProbe at the SOC were achieved using an ArF excimer laser system operating at a wavelength of 193 nm (4D Engineering, Hanover, Germany). The laser produces a beam size of 40 μm , has a pulse duration of 10 ns and an optimised repetition rate of 4 Hz. Ablated sample material is carried to the IsoProbe using a mixed He + Ar carrier gas. Analysis time was in the range 60–200 s. For the duration of the ablation the laser position and focus was fixed; no rastering was used. This typically gave total Hf signals of $7 \times 10^{-15} \text{ A } \mu\text{g g}^{-1} \text{ s}^{-1}$.

To investigate fractionation relationships and determine the isotopic abundance of Yb, we have used a VG Sector 54 thermal ionisation mass spectrometer (TIMS). REE solutions used in the experiments were measured in either static or dynamic collector arrays using ion beams generated from triple filament assemblies with Ta side and Re centre filaments.

Tail correction

It is recognised that the scatter of ions from a high abundance signal produces a ‘tail’ of extraneous ions across adjacent masses. This effect is proportional to the analyser vacuum condition^{13,16,17} and will induce a background over-correction if baselines are measured at inter-peak (half mass) positions. The tail effect is the contribution of the signal from a given peak at 1 Da on the low mass side, *e.g.*, the proportion of a ^{209}Bi ion beam measured at m/z 208. This abundance sensitivity is expressed in ppm and is generally proportional to the analyser vacuum (Fig. 1). If the analyser vacuum remains constant (*e.g.*, at $\sim 3 \times 10^{-8}$ mBar), the tail effect is a constant factor.

Abundance sensitivity measurements on the IsoProbe are approximately a factor of 3 higher than on the Nu Plasma,¹⁷ and as such the tail effect is significant and requires correction. We have determined the low and high mass tail effects on the IsoProbe across the Hf mass range by using ^{181}Ta and ^{169}Tm , respectively (Fig. 2). Signals measured at 0.5, 1.5, 2.5 and 3.5 Da away from 181 and 169 are used to interpolate the abundance sensitivity at 1–4 Da. The tail factors in the Hf isotope range on the low mass side are 8, 3, and 1 ppm at 1, 2,

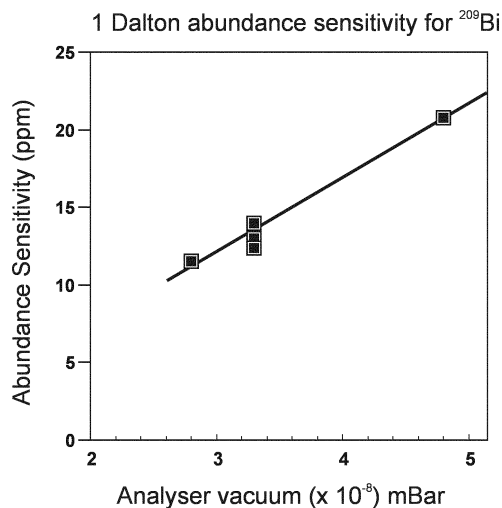


Fig. 1 Abundance sensitivity at m/z 208 relative to a ^{209}Bi signal under different analyser vacuum conditions.

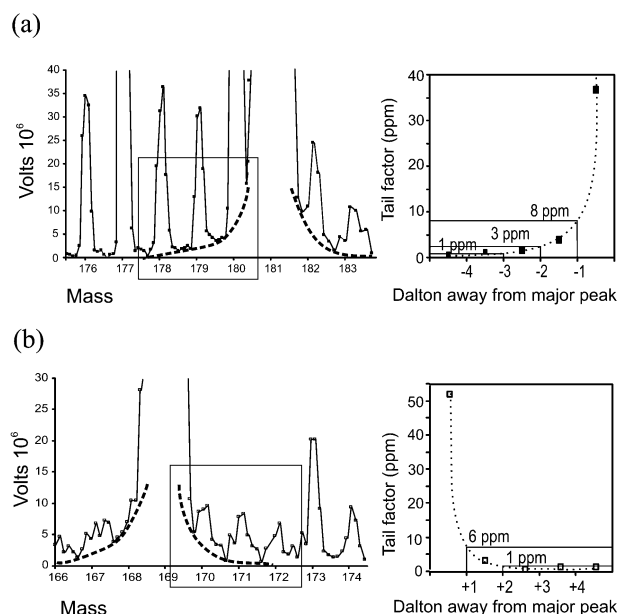


Fig. 2 Tail effects within the Hf mass range on the IsoProbe. Slow scan and half-mass measurements demonstrate the tail factor on (a) mass scan m/z 176–183 with a solution of $66 \mu\text{g l}^{-1} \text{ }^{181}\text{Ta}$, and (b) mass scan m/z 166–174 with a solution of $10 \mu\text{g l}^{-1} \text{ }^{169}\text{Tm}$. Inset graphs show the calculated abundance sensitivity (tail correction factors) interpolated from the scans.

and 3 Da, and on the high side are 6 and 1 ppm at 1 and 2 Da, respectively. During Hf measurement each mass is corrected for the tails of all other peaks, for example in the case of ^{176}Hf :

$$^{176}\text{Hf}_{\text{tailcorr}} = ^{176}\text{Hf}_{\text{meas}} - (^{177}\text{Hf} \times T_{L1} + ^{178}\text{Hf} \times T_{L2} + ^{179}\text{Hf} \times T_{L3}) - (^{175}\text{Lu} \times T_{H1} + ^{174}\text{Hf} \times T_{H2}) \quad (1)$$

where T_{L1} is the tail proportion expected at 1 Da light and T_{H1}

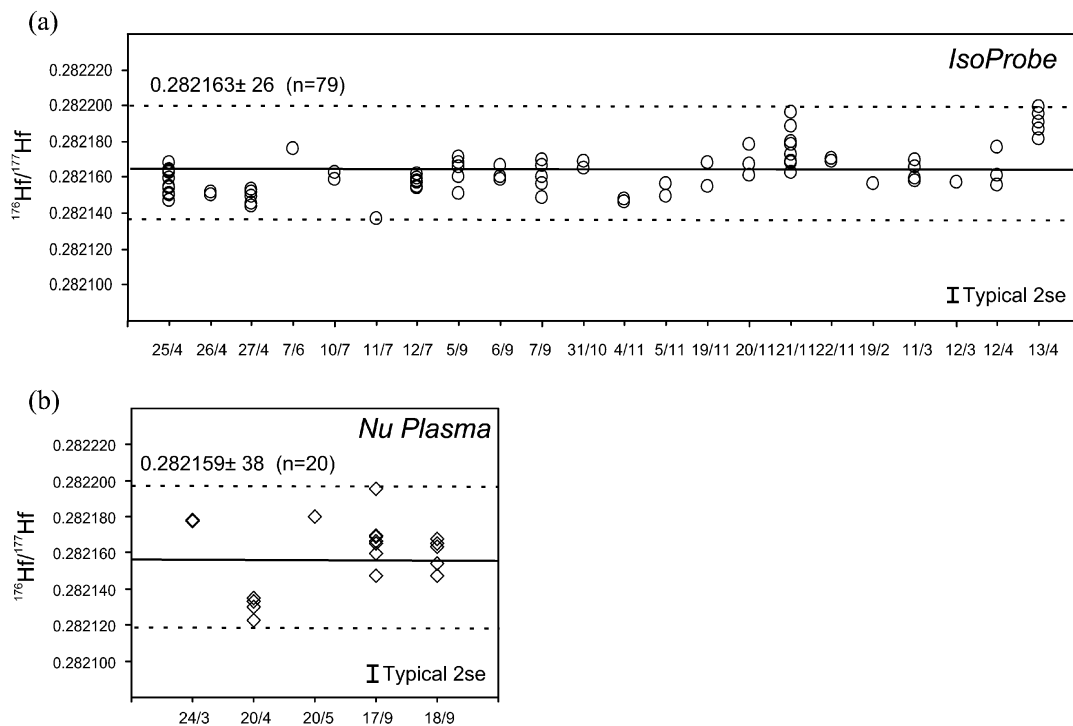


Fig. 3 (a) JMC 475 Hf standard measurement from April 2001 to April 2002 for the IsoProbe. The average from this study gives $^{176}\text{Hf}/^{177}\text{Hf} = 0.282163 \pm 26 (\pm 2\sigma_D, n = 79)$. (b) Equivalent measurements made on the Nu Plasma during the period March 2002 to September 2002. Average $^{176}\text{Hf}/^{177}\text{Hf} = 0.282159 \pm 38 (\pm 2\sigma_D; n = 20)$. For both instruments, each group of symbols represents one measuring day. Errors of individual analysis are typically $0.000007 (\pm 2 \text{ se})$.

is the tail at 1 Da heavy, and so on. The effects of tails are most significant where a low abundance isotope is close in mass to a high abundance isotope. In the Hf system this is particularly true for ^{175}Lu , which is adjacent to $^{176-178}\text{Hf}$.

Tail corrections on the Nu Plasma resulted in a 0.000003 shift in the $^{176}\text{Hf}/^{177}\text{Hf}$ result. This indicates that any errors resulting from the use of half-mass baselines are negligible as they are considerably smaller than the in-run errors on the measurements.

JMC 475 standard and rock standards

A solution of the JMC 475 Hf standard with concentrations of 40 ng ml^{-1} (IsoProbe) or 50 ng ml^{-1} (Nu Plasma) was used for instrumental set up and routine standard measurements. The $^{176}\text{Hf}/^{177}\text{Hf}$ ratio gives an average of $0.282163 \pm 26 (n = 79)$ ($\pm 2\sigma_D$) on the IsoProbe with good consistency over a 1-year measuring period, and $0.282159 \pm 38 (n = 20)$ ($\pm 2\sigma_D$; Fig. 3) on the Nu Plasma during 5 analytical sessions. The results of $^{176}\text{Hf}/^{177}\text{Hf}$ of the IsoProbe for a selection of international rock standards (BRR, BCR-1, BCR-2 and BE-N (Table 5)) fall within the range of published data.^{13,18–21}

Mass fractionation

In this study, we have assessed the instrumental mass bias using an exponential law:²²

$$R_t = R_m (M_B/M_A)^\beta \quad (2)$$

where R_m is the measured ratio of an isotope of exact mass M_B to an isotope with exact mass M_A , R_t is the accepted ratio of the two isotopes and hence β is the mass bias coefficient

$$\beta = \ln(R_m/R_t)/\ln(M_A/M_B) \quad (3)$$

β is calculated using an invariant isotope ratio with accepted values. In the case of the Hf system, $R_t = ^{179}\text{Hf}/^{177}\text{Hf} = 0.7325$.²³ Other measured Hf isotope ratios can be corrected for

mass bias using the β determined for $^{179}\text{Hf}/^{177}\text{Hf}$ (Table 6). This assumes that the bias across the Hf mass range can be described by the exponential law. In the case of Nd isotopes, the experimental relationship results in a slightly decreasing β value for ratios involving progressively heavier isotopes,¹ suggesting that the mass bias deviates marginally from the exponential law. Table 6 compares the proposed values with the values determined on the IsoProbe and Nu Plasma in this study. All ratios are similar, except for $^{178}\text{Hf}/^{177}\text{Hf}$, for which

Table 5 The $^{176}\text{Hf}/^{177}\text{Hf}$ values of international rock reference samples measured in this study in comparison with previously published values^a

	$^{176}\text{Hf}/^{177}\text{Hf}$ (2 se)	Reference
BRR ^b	0.283368 ± 10	This study ^c
	0.283366 ± 8	This study
	0.283368 ± 16	Kempton <i>et al.</i> (2000)
	0.283351 ± 16	Kempton <i>et al.</i> (2000)
	0.283363 ± 16	Average $\pm 2 \text{ sd}$
BCR-1	0.282845 ± 10	This study
	0.282866 ± 9	This study
	0.282860 ± 11	David <i>et al.</i> (2001)
	0.282817 ± 8	Le Fèvre and Pin (2001)
	0.282879 ± 8	Blichert-Toft (2001)
BCR-2	0.282892 ± 6	Münker <i>et al.</i> (2001)
	0.282860 ± 53	Average $\pm 2 \text{ sd}$
	0.282859 ± 9	This study
	0.282884 ± 7	Le Fèvre and Pin (2001)
	0.282872 ± 35	Average $\pm 2 \text{ sd}$
BE-N	0.282929 ± 12	This study
	0.282939 ± 4	Münker <i>et al.</i> (2001)
	0.282923 ± 9	Münker <i>et al.</i> (2001)
	0.282921 ± 6	Münker <i>et al.</i> (2001)
	0.282921 ± 7	Blichert-Toft (2001)
	0.282927 ± 15	Average $\pm 2 \text{ sd}$

^aAll $^{176}\text{Hf}/^{177}\text{Hf}$ data are reported relative to 0.282160 for JMC-475.

^bBRR is identical to sample CD80-WP02-D6 in ref. 18; SOC standard—Basalt Reykjanes Ridge, $1.5 \mu\text{g g}^{-1}$ Hf. ^cAll rock standard data acquired for this study were made using the IsoProbe.

Table 6 Hf isotopic composition values for JMC 475 from the literature and this study

	Patchett ³¹ (ID-TIMS) ^a		Blichert-Toft <i>et al.</i> ^{6b}	Kleinhanns <i>et al.</i> ³³	This study (± 2 sd)		This study (± 2 sd)	
	IUPAC (1998)	<i>n</i>	TIMS/P54	(Nu Plasma)	(IsoProbe)	<i>n</i>	(Nu Plasma)	<i>n</i>
¹⁷⁴ Hf/ ¹⁷⁷ Hf	0.008710 \pm 50	25	N/A		0.008674 \pm 32	41	N/A	
¹⁷⁶ Hf/ ¹⁷⁷ Hf	0.282195 \pm 15	25	0.28216	0.282169 \pm 16	0.282163 \pm 26	79	0.282159 \pm 38	20
¹⁷⁸ Hf/ ¹⁷⁷ Hf	1.467100 \pm 100	25	1.467168	1.467290 \pm 80	1.467417 \pm 232	79	1.467304 \pm 147	20
¹⁷⁹ Hf/ ¹⁷⁷ Hf	0.732500		0.732500		0.732500		0.732500	
¹⁸⁰ Hf/ ¹⁷⁷ Hf	1.886510 \pm 120	25	1.886666	1.88680 \pm 30	1.886765 \pm 290	75	1.886683 \pm 625	20

^aThe author has suggested a baseline interference by Re and some values may not be final. ^bNo error value was reported.

Table 7 Yb isotopic composition values

	TIMS/P54 ^{6,9}	IUPAC (1998) ²⁴	This study ± 2 sd (TIMS)	<i>n</i>	This study (IsoProbe)	<i>n</i>
¹⁶⁸ Yb/ ¹⁷¹ Yb	0.00951	0.00889	0.008865 \pm 22	2	0.008845 \pm 63	19
¹⁷⁰ Yb/ ¹⁷¹ Yb	0.2137	0.21289	0.212645 \pm 6	2	0.212531 \pm 49	19
¹⁷² Yb/ ¹⁷¹ Yb	1.5264	1.52871	1.532075 \pm 272	6	1.532227 \pm 75	19
¹⁷³ Yb/ ¹⁷¹ Yb	1.1248	1.12955	1.132685		1.132685	
¹⁷⁴ Yb/ ¹⁷¹ Yb	2.2163	2.22899	2.242466 \pm 160	6	2.242716 \pm 266	19
¹⁷⁶ Yb/ ¹⁷¹ Yb	0.8859	0.89356	0.901821 \pm 189	4	0.901864 \pm 508	19
¹⁷⁶ Lu/ ¹⁷⁵ Lu	0.02656	0.026512	0.026549		N/A	

results from both instruments in this study are slightly higher (~ 0.000200) than published values.

Interference correction of Hf isotopes

To obtain accurate ¹⁷⁶Hf/¹⁷⁷Hf, isobaric interferences from ¹⁷⁶Lu and ¹⁷⁶Yb must be accounted for. Using interference-free masses, *i.e.* ¹⁷⁵Lu and ¹⁷³Yb or ¹⁷¹Yb, interferences can be subtracted according to their accepted isotopic abundances of 0.02656 for ¹⁷⁶Lu/¹⁷⁵Lu and 0.7876 for ¹⁷⁶Yb/¹⁷³Yb or 0.8859 for ¹⁷⁶Yb/¹⁷¹Yb (Table 7). The mass 176 isobaric interference correction functions can be expressed as

$$^{176}\text{Hf} = 176_{\text{m}} - \left[^{175}\text{Lu} \times \left(\frac{^{176}\text{Lu}/^{175}\text{Lu}}{M_{176}/M_{175}} \right)^{\beta(\text{Lu})} + ^{173}\text{Yb} \times \left(\frac{^{176}\text{Yb}/^{173}\text{Yb}}{M_{176}/M_{173}} \right)^{\beta(\text{Yb})} \right] \quad (4)$$

In this study, we have used a series of Yb-doped JMC 475 Hf solutions, so that the total Yb/Hf ranged between 0.0002 and 0.05, to evaluate the capability of the interference corrections on both the IsoProbe and the Nu Plasma. The results of these experiments are described below.

The mass bias relationship between Yb and Hf

If plasma ion sources provide similar levels of ionisation of elements with similar masses then it is plausible to use the measured Hf mass bias to correct the bias within the interfering elements, Yb and Lu (*i.e.*, assuming $\beta_{\text{Hf}} = \beta_{\text{Lu}} = \beta_{\text{Yb}}$ in eqn. 3). Fig. 4(a) shows the ¹⁷⁶Hf/¹⁷⁷Hf measurements of the Yb–Hf mixtures corrected using the Yb isotope abundances of McCulloch *et al.*⁹ and Blichert-Toft *et al.*⁶ using various mass bias schemes for Yb. The crossed symbols are Hf measurements corrected for Yb interference assuming no mass bias of Yb (*i.e.*, $\beta_{\text{Yb}} = 0$ in eqn. 4). Solid symbols denote ¹⁷⁶Hf/¹⁷⁷Hf corrected for Yb interference using β_{Hf} from ¹⁷⁹Hf/¹⁷⁷Hf (*i.e.*, $\beta_{\text{Yb}} = \beta_{\text{Hf}}$). In the case where no mass bias correction is used, both instruments show a marked positive correlation between ¹⁷⁶Hf/¹⁷⁷Hf and Yb/Hf. Positive trends are also produced on the instruments where β_{Hf} is applied to Yb. This suggests two possibilities: firstly, that $\beta_{\text{Yb}} \neq \beta_{\text{Hf}}$ due to a difference in the way these elements ionise, or secondly that the isotope abundances used in calculating the β values for one of the two elements are inappropriate.

To investigate this further we have obtained an empirical Yb and Hf mass bias relationship by measuring mixtures of Hf-free Yb solution (SPEX ‘Assurance’, ICP standard solution) and

the JMC475 Hf standard with Yb/Hf = 1 and Yb/Hf = 0.3. β values measured for Hf and Yb in these mixtures are shown as the open symbols (squares for IsoProbe; circles for Nu Plasma) in Fig. 5. Nu Plasma β values are lower than those obtained on the IsoProbe, but data from both instruments lie approximately on a line passing through the origin, which is shown as a dashed line in Fig. 5. The correlation has the form:

$$\beta(^{173}\text{Yb}/^{171}\text{Yb}) = 1.272 \times \beta(^{179}\text{Hf}/^{177}\text{Hf}) \quad (5)$$

From this equation it is clear that β_{Yb} is apparently greater than β_{Hf} , which would lead to the under correction of the ¹⁷⁶Yb and produce an overly radiogenic Hf isotope ratio in analyses where Yb is present. It should also be noted that the trends produced by each instrument from variations in mass bias cut across the overall correlation line (Fig. 5). The relationship of β_{Hf} to β_{Yb} given by this line could potentially be used to correct the Yb mass bias in the determination of ¹⁷⁶Hf/¹⁷⁷Hf. Results of this correction procedure on the range of mixed Hf–Yb solutions are shown as the open symbols in Fig. 4(a). Over the range of mixtures used, the ¹⁷⁶Hf/¹⁷⁷Hf is invariant within error, indicating a satisfactory correction.

Despite the success of the empirical correction, it does not solve the question as to whether the results from Hf–Yb mixtures are a product of differing ionisation of the two elements or are related to inappropriate isotopic abundances. To test this further we have investigated Yb isotope abundances using TIMS.

Yb isotope abundances measured on TIMS

Yb isotope abundances have been measured previously by McCulloch *et al.*⁹ using ID-TIMS, by Holliger and Devillers²⁴ using TIMS and Blichert-Toft *et al.*⁶ using MC-ICP-MS. The IUPAC values currently accepted are those of Holliger and Devillers.²⁴ It has been suggested by laser ablation studies^{7,8} that the ¹⁷⁶Yb/¹⁷¹Yb and ¹⁷⁶Yb/¹⁷³Yb accepted ratios may be too low. We have carried out a series of TIMS measurements to attempt to evaluate the validity of the currently accepted Yb isotopic ratios. To do this we have utilised other rare earth elements, Nd and Ce, which have well constrained isotopic abundances^{25,26} based on the analysis of gravimetric compounds or rigorous examination for geochronological measurements. These elements are used here as analogues of the fractionation behaviour of Yb during thermal ionisation.

It is recognised that in TIMS analysis pure fractions of

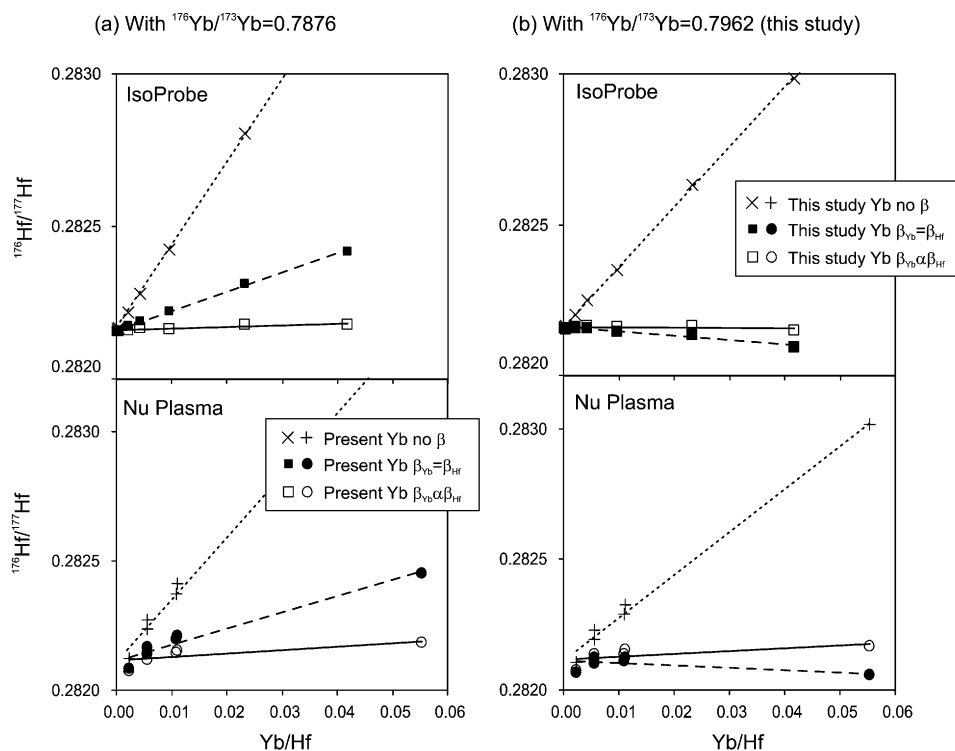


Fig. 4 (a) $^{176}\text{Hf}/^{177}\text{Hf}$ plotted against Yb/Hf for mixtures of JMC475 and Yb. Upper plot for the IsoProbe; lower plot for the Nu Plasma. Symbols ‘+’ and ‘x’ represent ^{176}Yb corrected using natural $^{173}\text{Yb}/^{176}\text{Hf}$; closed symbols (squares or circles) are ^{176}Yb corrected using $\beta_{\text{Yb}} = \beta_{\text{Hf}}$, and open squares or circles are ^{176}Yb corrected using $\beta_{\text{Yb}} = 1.272 \times \beta_{\text{Hf}}$ (eqn. 5, Fig. 5, dashed line). (b) The same corrections but with the new proposed Yb isotope values (Table 7).

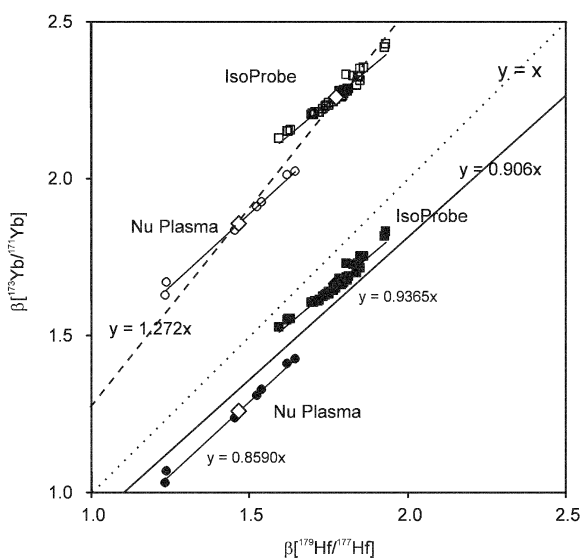


Fig. 5 $\beta(^{179}\text{Hf}/^{177}\text{Hf})$ plotted against $\beta(^{173}\text{Yb}/^{171}\text{Yb})$. Open squares/circles are individual Hf–Yb measurements with the present Yb isotope values (Table 7, TIMS/P54) on the IsoProbe and Nu Plasma, respectively. The correlation derived from present Yb values is presented in a dashed line as $y = 1.272x$. Closed squares/circles are the same measurements using the new Yb values from this study; they are parallel to the correlation line.

elements consistently produce light isotope enriched ratios during the initial stages of ionisation at a given temperature and sample quantity on the filament. This is one of the fundamental principals of external fractionation correction of Pb isotopes used through the last 40 years. The use of double spike Pb techniques on TIMS has superseded the external fractionation correction as the method of choice^{16,27} but within the errors of the external correction technique, good estimates of the level of fractionation can be achieved. In the case of Nd,

large sample loads ($\sim 1 \mu\text{g}$) of purified Nd result in $^{146}\text{Nd}/^{144}\text{Nd}$ ratios that focus around a particular value, particularly during the initial stages of the ionisation.

We have examined 37 measurements of Nd isotopic standards (JMC321, La Jolla and JNdi) with Nd loads in excess of 500 ng. During the first 15 min of measurement (30 ratios) the average $^{146}\text{Nd}/^{144}\text{Nd} = 0.719433 \pm 0.00139$ (2 se), which is lighter than the accepted value of $^{146}\text{Nd}/^{144}\text{Nd}$ (0.7219), and equates to a β value of -0.248 (Table 8). These measurements, performed over a period of 6 years, conform to the typical light to heavy thermal fractionation progression. A similar comparison for Ce isotopes using the $^{138}\text{Ce}/^{142}\text{Ce}$ produces a β value of -0.219 , indicating that the level of initial fractionation is similar between these elements, despite variations in their first ionisation potentials. If we assume that the behaviour of Yb using identical analytical protocols is comparable to that of Nd and Ce, we can apply the β value generated from the other rare earths to correct the measured Yb isotope ratios. Taking $^{173}\text{Yb}/^{171}\text{Yb}$ as a reference, we have taken the average initial value measured on the TIMS (1.129416) and fractionation corrected it using $\beta = -0.248$ to give $^{173}\text{Yb}/^{171}\text{Yb} = 1.132685$. Using this as a normalising ratio (*i.e.*, as R_i in eqn. 2) the other Yb ratios can be internally corrected for fractionation. The resulting ratios are presented in Table 8. Using the same $^{173}\text{Yb}/^{171}\text{Yb}$ value, Yb ratios measured on the MC-ICP-MS instruments are normalised in the same way and are shown for comparison in Table 7.

Table 8 Exponential deviation of accepted values and initial thermal ionisation results

HREE isotope pair	Accepted values (ref.)	Initial ionisation average ^a ± 2 se	<i>n</i>	β
$^{146}\text{Nd}/^{144}\text{Nd}$	0.7219 (25)	0.719433 ± 139	37	-0.248
$^{136}\text{Ce}/^{142}\text{Ce}$	0.01688 (26)	0.017080 ± 61	2	-0.272

^aThe ratios were taken from the first 15 min of the ionisations during TIMS analysis.

The Yb isotope ratios calculated in this thermal ionisation experiment can now be applied to the Hf–Yb measurements. These are plotted as solid symbols in Fig. 5, and lie much closer to the $\beta_{\text{Hf}} = \beta_{\text{Yb}}$ line than data calculated using the currently accepted Yb ratios. Furthermore, the data from each instrument lie parallel to, rather than across, lines intersecting the origin. In a similar fashion, the new Yb ratios can be applied to the series of Hf–Yb mixtures, the recalculations of which are shown in Fig. 4(b). In this plot the crossed symbols, where $\beta_{\text{Yb}} = 0$, define a positive trend. The solid squares, where $\beta_{\text{Yb}} = \beta_{\text{Hf}}$, lie close to a constant $^{176}\text{Hf}/^{177}\text{Hf}$, but with a slight tendency to decreasing $^{176}\text{Hf}/^{177}\text{Hf}$ with increasing Yb content in the mixture. This could suggest that the revised values for Yb defined in this study are slightly offset, or that a difference does exist between the mass bias of Hf and Yb. The subtly different behaviour of Yb and Hf is the most likely explanation as data from each of the instruments used in this study lie on a different trend in Fig. 5, with different Hf coefficients (0.9365 for the IsoProbe and 0.8590 for the Nu Plasma). A comparison between the Yb and Hf mass bias across the two isotope systems is displayed in Fig. 6. This figure shows mass bias for a range of Yb and Hf isotope pairs, and plots the β values against the average mass of the pair. It shows that the β_{Yb} generated using the Yb abundances determined in this study produce (1) similar β values for Hf and Yb, (2) roughly consistent β values across the Yb mass range and (3) a slight increase in the mass bias (higher β_{Yb}) with decreasing mass. This contrasts with the β_{Yb} generated using the existing values, which are shown as open squares in Fig. 6. These show a scatter of β across the Yb mass range, and significantly higher mass bias of Yb relative to Hf. Differences in mass bias between elements across a large range in masses is clearly recognised in MC-ICP-MS instruments.^{28,29} β values on the IsoProbe for a range of masses are U \sim 1.2, Pb \sim 1.3, Hf \sim 1.9, Nd \sim 2.3, and Sr \sim 2.5. However,

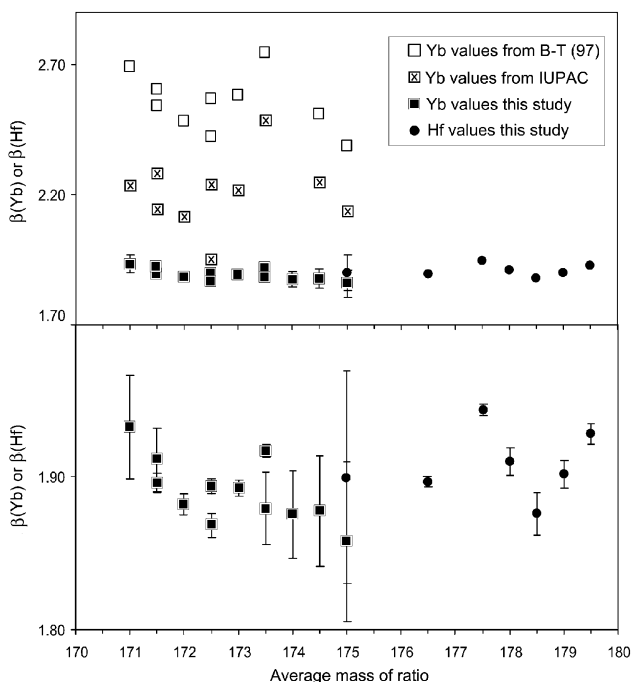


Fig. 6 Variations of the exponential mass bias function β relative to the average mass of $M_A - M_B$ for the Yb and Hf isotope systems (the lower plot has an expanded scale). Analyses were carried out separately during the same analysis session with single element solutions. The three sets of square symbols are β values for Yb derived from various Yb values (open squares from McCulloch *et al.*³⁰ and Blichert-Toft *et al.*⁶; crossed squares from Holliger and Devillers,²⁴ and closed squares from this study, Table 7) and closed circles are those for Hf. Some mass averages are derived from 2 sets of isotope ratios, *i.e.* $^{174}\text{Yb}/^{173}\text{Yb}$ and $^{176}\text{Yb}/^{171}\text{Yb}$: both result in an average of 173.5.

slight increases in bias towards lower mass ratios have also been observed in the isotopic spectrum of individual elements,¹ which may be the case for the Yb data presented in this study.

The discrepancy between the Hf–Yb mixtures corrected using $\beta_{\text{Hf}} = \beta_{\text{Yb}}$ and a constant $^{176}\text{Hf}/^{177}\text{Hf}$ (Fig. 4(b), closed symbols) can be adjusted using a correction developed in a similar way to eqn. 5, except that the level of adjustment is smaller. The result of this additional correction is shown in Fig. 4(b) as the open symbols.

Lu can be investigated in a similar fashion to Yb. Values suggested for $^{176}\text{Lu}/^{175}\text{Lu}$ vary considerably,^{24,30,31} including the commonly used value of 0.02656.⁶ This variation is related to the difficulty in determining the Lu isotopic ratio since only two isotopes exist in nature and the proportion of ^{176}Lu is very small (2.59%). Fractionation analyses performed on TIMS and adjusted in the same way as Yb produce a ratio of 0.02655 (Table 7), which is close to the present recommended value.⁶ Fig. 7 shows the $\beta_{\text{Lu}} - \beta_{\text{Hf}}$ correlation based on the measurement of a 1:1 Hf: Lu solution and the $^{176}\text{Lu}/^{175}\text{Lu} = 0.02655$ ratio. The results, shown as diamonds in Fig. 7, form an array displaced from the $\beta_{\text{Lu}} = \beta_{\text{Hf}}$ correlation (Fig. 7, diamond symbols), with $\beta_{\text{Lu}} = 0.7966 \times \beta_{\text{Hf}}$. This is surprising given the equivalence of β_{Yb} and β_{Hf} generated by our experiments in this study. It is unlikely that the R_t of $^{176}\text{Lu}/^{175}\text{Lu}$ is in error as a value of \sim 0.02647 would be required to generate $\beta_{\text{Lu}} = \beta_{\text{Hf}}$, which is lighter than any initial stage TIMS values. It is therefore likely that the measurement of Lu in the presence of equivalent amounts of Hf on the plasma source instruments is the source of the problem, as large corrections have to be made for the isobaric ^{176}Hf on the ^{176}Lu . In most natural samples the Lu content is about an order of magnitude lower than the Yb and Hf and thus the correction is relatively small.

Yb correction of laser ablation analysis by MC-ICP-MS

For comparison, the Yb and Hf mass bias relationship described above was tested using laser ablation as an alternate sample introduction method. The NIST SRM 610 glass

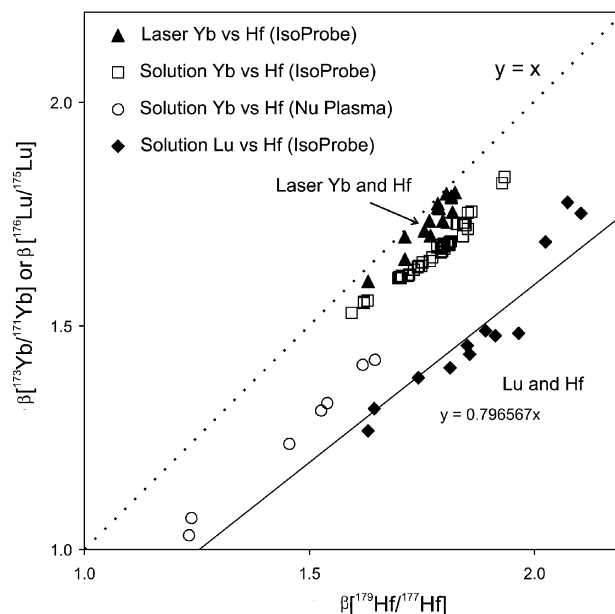


Fig. 7 $\beta(^{176}\text{Lu}/^{175}\text{Lu})$ and $\beta(^{173}\text{Yb}/^{171}\text{Yb})$ versus $\beta(^{179}\text{Hf}/^{177}\text{Hf})$ for solution and laser ablation analysis. Laser determinations are from NIST SRM 610 glass standard ($416.5 \mu\text{g g}^{-1}$ Yb, $417.7 \mu\text{g g}^{-1}$ Hf); solution measurements are those from Fig. 5, corrected using the Yb values proposed in this study, and JMC 475 Hf doped with pure Lu, where Lu/Hf = 0.5. Closed triangles are the laser ablation results of Yb and Hf correlations, which fall within same range as samples introduced by solution. The Lu and Hf correlation is slightly below that of Yb and Hf.

standard, containing Hf 417.7 $\mu\text{g g}^{-1}$, Yb 416.5 $\mu\text{g g}^{-1}$,³² was ablated and analysed using the IsoProbe MC-ICP-MS. The results are shown in Fig. 7 as solid triangles. The $\beta_{\text{Hf}}-\beta_{\text{Yb}}$ covariation from the laser analysis is close to the range of values generated by solution nebulisation on the same instrument (open squares), but lies slightly closer to the $\beta_{\text{Hf}} = \beta_{\text{Yb}}$ line. The differences between the solution and laser mass bias are likely to be small as both introduction methods present the plasma with sample in the form of a dry aerosol. Although the signal levels generated by laser are lower, these results indicate that a similar correction procedure to the solution analysis can be applied.

Conclusions

In this study we have examined the relationship between Yb and Hf mass bias with a view to improving isobaric interference corrections. Two different MC-ICP-MS instruments (IsoProbe and Nu Plasma) demonstrate that if currently accepted values for Yb isotope ratios are employed in the corrections, large deviations in $^{176}\text{Hf}/^{177}\text{Hf}$ are found in solutions with increasing Yb/Hf ratios. Using thermal ionisation mass spectrometry we have defined an internally consistent set of Yb isotope ratios that were tested as an independent calibration of the plasma source results. Using the new values, it can be concluded that Yb and Hf have similar levels of mass bias and that consistent $^{176}\text{Hf}/^{177}\text{Hf}$ can be achieved following the application of a simple empirical correction. Laser ablation sample introduction demonstrates that the same Yb correction is potentially applicable to the analysis of solid samples where chemical separations are not possible.

Acknowledgements

We thank Takafumi Hirata for fruitful discussions that greatly improved a previous manuscript. We are also grateful for the comments provided by anonymous reviewers. G. B. thanks Nathalie Vigier and Peter van Calsteren for assistance with the Nu Plasma. Funding for this study was provided to N.-C. C. by Micromass UK and the University of Southampton Taiwanese Postgraduate Scholarship. The IsoProbe at the SOC was funded through the PRISMS project (EC contract SMT4-CT98-2220). Analysis on the Nu Plasma was supported by a Postdoctoral Fellowship of the Open University (G. B.).

References

- 1 D. Vance and M. F. Thirlwall, *Chem. Geol.*, 2002, **185**, 227.
- 2 H. P. Longerich, B. J. Fryer and D. F. Strong, *Spectrochim. Acta*, 1987, **42B**, 39.
- 3 C. N. Maréchal, P. Telouk and F. Albarède, *Chem. Geol.*, 1999, **156**, 251.
- 4 W. M. White, F. Albarède and P. Telouk, *Chem. Geol.*, 2000, **167**, 257.
- 5 B. Luais, P. Telouk and F. Albarède, *Geochim. Cosmochim. Acta*, 1997, **61**, 4847.
- 6 J. Blichert-Toft, C. Chauvel and F. Albarède, *Contrib. Mineral. Petrol.*, 1997, **127**, 248.
- 7 M. F. Thirlwall and A. J. Walder, *Chem. Geol.*, 1995, **122**, 241.
- 8 L. Griffin, N. J. Pearson, E. Belousova, S. E. Jackson, E. van Achterbergh, S. Y. O'Reilly and S. R. Shee, *Geochim. Cosmochim. Acta*, 2000, **64**, 133.
- 9 M. T. McCulloch, K. J. R. Rosman and J. R. De Laeter, *Geochim. Cosmochim. Acta*, 1977, **41**, 1703.
- 10 P. J. De Bièvre, M. Gallet, N. E. Holden and I. L. Barnes, *J. Phys. Chem. Ref. Data*, 1984, 13.
- 11 J. Blichert-Toft and F. Albarède, *Earth Planet. Sci. Lett.*, 1997, **148**, 243.
- 12 D.-C. Lee, A. N. Halliday, J. R. Hein, K. W. Burton, J. N. Christensen and D. Gunther, *Science (Washington, D. C.)*, 1999, **285**, 1052.
- 13 C. Münker, S. Weyer, E. E. Scherer and K. Mezger, *Geochem., Geophys., Geosyst.*, 2001, **2**, Paper number 2001GC000183.
- 14 R. N. Taylor, T. Warneke, J. A. Milton, I. W. Croudace, P. E. Warwick and R. W. Nesbitt, *J. Anal. At. Spectrom.*, 2001, **16**, 279.
- 15 N. S. Belshaw, P. A. Freedman, R. K. O'Nions, M. Frank and Y. Guo, *Int. J. Mass Spectrom.*, 1998, **181**, 51.
- 16 M. F. Thirlwall, *Chem. Geol.*, 2000, **163**, 299.
- 17 M. F. Thirlwall, *J. Anal. At. Spectrom.*, 2001, **16**, 1121.
- 18 P. D. Kempton, J. G. Fitton, A. D. Saunders, G. M. Nowell, R. N. Taylor, B. S. Hardarson and G. Pearson, *Earth Planet. Sci. Lett.*, 2000, **177**, 255.
- 19 J. Blichert-Toft, *Geostand. Newsl.*, 2001, **25**, 41.
- 20 K. David, M. Frank, R. K. O'Nions, N. S. Belshaw, J. W. Arden and J. Hein, *Chem. Geol.*, 2001, **178**, 23.
- 21 B. Le Fèvre and C. Pin, *Anal. Chem.*, 2001, **73**, 2453.
- 22 W. A. Russell, D. A. Papanastassiou and T. A. Tombrello, *Geochim. Cosmochim. Acta*, 1978, **42**, 1075.
- 23 P. J. Patchett and M. Tatsumoto, *Contrib. Mineral. Petrol.*, 1980, **75**, 263.
- 24 P. Holliger and C. Devillers, *Earth Planet. Sci. Lett.*, 1981, **52**, 76.
- 25 G. J. Wasserburg, S. B. Jacobsen, D. J. DePaolo, M. T. McCulloch and T. Wen, *Geochim. Cosmochim. Acta*, 1981, **45**, 2311.
- 26 A. Makishima, H. Shimizu and A. Masuda, *Mass. Spectrosc.*, 1987, **35**, 64.
- 27 S. J. G. Galer and W. Abouchami, *Mineral. Mag.*, 1998, **62A**, 491.
- 28 T. Hirata, *Analyst*, 1996, **121**, 1407.
- 29 M. Rehkämper, M. Schönbächler and C. H. Stirling, *Geostand. Newsl.*, 2001, **25**, 23.
- 30 M. T. McCulloch, J. R. De Laeter and K. J. R. Rosman, *Earth Planet. Sci. Lett.*, 1976, **28**, 308.
- 31 P. J. Patchett, *Geochim. Cosmochim. Acta*, 1983, **47**, 81.
- 32 N. J. G. Pearce, W. T. Perkins, J. A. Westgate, M. P. Gorton, S. E. Jackson, C. R. Neal and S. P. Chenery, *Geostand. Newsl.*, 1997, **21**, 115.
- 33 I. C. Kleinhans, K. Kreissig, B. S. Kamber, T. Meisel, T. F. Nägler and J. D. Kramers, *Anal. Chem.*, 2002, **74**, 67.